

Federated Learning of Shareable Bases for Personalization-Friendly Image Classification

Hong-You Chen^{1*†} Jike Zhong^{1*} Mingda Zhang² Xuhui Jia²
 Hang Qi² Boqing Gong² Wei-Lun Chao¹ Li Zhang²

¹The Ohio State University ²Google Research

Abstract

Personalized federated learning (PFL) aims to harness the collective wisdom of clients’ data while building personalized models tailored to individual clients’ data distributions. Existing works offer personalization primarily to clients who participate in the FL process, making it hard to encompass new clients who were absent or newly show up. In this paper, we propose FEBASIS, a novel PFL framework to tackle such a deficiency. FEBASIS learns a set of few shareable “basis” models, which can be linearly combined to form personalized models for clients. Specifically for a new client, only a small set of combination coefficients, not the model weights, needs to be learned. This notion makes FEBASIS more parameter-efficient, robust, and accurate than competitive PFL baselines, especially in the low data regime, without increasing the inference cost. To demonstrate the effectiveness and applicability of FEBASIS, we also present a more practical PFL testbed for image classification, featuring larger data discrepancies across clients in both the image and label spaces as well as more faithful training and test splits.

1 Introduction

Recent years have witnessed a gradual shift in machine learning towards taking users’ aspects into account. Building personalized models (e.g., image classifiers) tailored to users’ data, preferences, and characteristics has been shown to improve user experience greatly (Rudovic et al. 2018).

To achieve so, however, may sacrifice data privacy and ownership during the collection of training data, as highlighted in (Jordan and Mitchell 2015; Papernot et al. 2016). Personalized federated learning (PFL) is a promising machine learning paradigm that can fulfill the demands of both worlds (Tan et al. 2022). On the one hand, it strictly follows the setup of federated learning (FL): training models collaboratively with multiple users (i.e., clients) while keeping their data decentralized (Kairouz et al. 2019). On the other hand, it personalizes models for clients that feature better accuracy in their respective data distributions.

Despite making promising progress, existing works of PFL mostly limit their personalization capability to clients who participate in the FL process. For example, mainstream

methods based on multi-task learning (Li et al. 2020; Smith et al. 2017) jointly train models for clients to prevent overfitting. For a new client who was not involved in the previous FL process, there is no clear principle to construct a personalized model except for conducting another run of the FL process. This deficiency greatly limits the applicability of PFL in practice, especially for a personalization service provider: new clients may show up at any time, and it is extremely inefficient to rerun the FL process every time.

At first glance, one may resolve this problem by first training a global model with participating clients (e.g., via FEDAVG (McMahan et al. 2017)) and then fine-tuning it for each new client. However, it has two noticeable drawbacks. First, fine-tuning an over-parameterized neural network with limited data, which is often the case for new clients, is known to be sensitive to hyperparameters and prone to overfitting (Li et al. 2021a; Pillutla et al. 2022; Wu et al. 2022; Fallah, Mokhtari, and Ozdaglar 2020). Second, fine-tuning a single global model prevents us from leveraging the diversity and relationships of the participating clients to facilitate personalization for new clients.

In this paper, we, therefore, strive to tackle a novel PFL problem: *how to learn and leverage knowledge from participating clients in the past to facilitate personalization for new clients, especially in the low data regime?*

We make a mild assumption: the data distribution of a new client is covered by the aggregated data distribution of all the participating clients. More precisely, treating each client as a “point” in the “client space”, we assume that a new client is located on or near the subspace spanned by the participating clients. Under this assumption, we propose a novel “personalization-friendly” PFL framework called FEBASIS, which goes beyond learning personalized models for participating clients (i.e., point estimates) toward learning the underlying subspace of clients’ models so that we can rapidly and robustly construct personalized models for new clients. Concretely, FEBASIS learns *a few shareable “basis” models* of the same architecture to capture the subspace spanned by clients, inspired by (Changpinyo et al. 2016; Evgeniou and Pontil 2007). With these basis models, we can synthesize a client model by a linear (more strictly, convex) combination estimated on the fly. Fig. 1 gives an illustration.

Despite its conceptual simplicity, FEBASIS has several notable advantages for PFL. First, FEBASIS is reminis-

*These authors contributed equally.

†Partial work done as a research intern at Google Research.
 Preprint. All rights reserved.

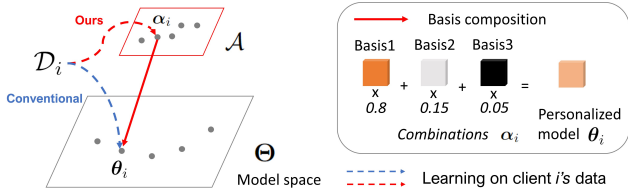


Figure 1: In conventional PFL methods, *each client* learns a *high-dimensional model* (blue) on its dataset \mathcal{D}_i . In **our FEDBASIS**, we learn a few shareable basis models of the same neural network architecture on the participating clients. After the basis models are trained, a *new client* only needs to learn a *low-dimensional vector* (red) as the coefficients to combine them into a personalized network, making **FEDBASIS** more data-efficient and robust for supporting new clients, i.e., more “personalization-friendly.”

cent of dictionary learning (Mairal et al. 2009) in the neural network’s parameter space. That is, **FEDBASIS** reduces the overall learnable parameters by summarizing the participating clients’ models into the basis models, effectively reducing the sample complexity in federated learning. Second, when a new client arrives, **FEDBASIS** learns the combination coefficients, not the model weights, to construct a personalized model, making it more robust to the low data regime. Importantly, **FEDBASIS** combines the parameters of the basis models, not their predictions (sharply different from the mixture of experts (Reisser et al. 2021)). As such, the inference cost remains almost the same as a single neural network model and does not scale with the number of bases.

To ensure that the basis models learn diverse knowledge in a federated setting to support a variety of client distributions¹, we propose a *coordinate descent* style model update. During each round of local training, we first update the combination coefficients alone, freeze and sharpen them (so most elements are near zero), and perform SGD solely on the basis models for multiple epochs. The sharpening operation limits the bases each client can use and, in turn, forces different bases to learn from different subsets of clients, leading to basis models that capture diverse specialized knowledge.

To support more realistic and faithful PFL evaluation, as a side contribution, we construct a new set of benchmark datasets, **PFLBED**. The motivations for **PFLBED** are two-fold. First, **PFLBED** is carefully designed to minimize the mismatch between the training and testing distributions for each client. To our surprise, we found such a mismatch huge in existing datasets (Caldas et al. 2018; Li et al. 2021a), which may mislead the progress of PFL. Second, we consider more challenging non-IID conditions across clients, capturing variations in both the data and label distributions, in contrast to many existing datasets that focus on merely one of them (Chen and Chao 2022; Sun et al. 2021).

We validate **FEDBASIS** on both the standard PFL datasets and **PFLBED** for constructing personalized models for new clients. Compared to mainstream PFL approaches, **FEDBASIS** achieves more robust performance across various PFL settings, demonstrating its superiority for personalization.

¹In an FL setting which involves local model training with each client’s data alone, we found it challenging to learn diverse basis models — the bases easily collapse into non-specialized models.

2 Related Work

Conventional PFL is quite well-studied for clients who participate in the federated learning process. Differently, we focus on a less explored problem that aims to construct personalized models for individual new clients, which was first raised briefly in (Shamsian et al. 2021; Collins et al. 2021).

Conventional PFL. Many earlier works formulate personalization with multiple clients as *multi-task learning (MTL)* and focus on regularizer designs while each client learns its own model (Smith et al. 2017; Zhang et al. 2021a; Li et al. 2021a; Dinh, Tran, and Nguyen 2020). *Mixture of models* (Zec et al. 2020; Marfoq et al. 2021; Luo and Wu 2022; Ruan and Joe-Wong 2022) assumes the clients’ data are from a mixture of distributions. It then learns a global model and a set of local models and takes a mixture of them in their outputs (not the model weights like ours) to perform personalized predictions. *Clustered FL* (Ghosh et al. 2020) relies on a rather strong assumption that the clients are grouped into a few clusters and share one model per cluster.

General / generalized representations. More recent approaches rely on a universal feature extractor. Each client only personalizes an output head (Collins et al. 2021; Chen and Chao 2022), a Gaussian process tree classifier (Achituv et al. 2021), or a k -NN classifier (Marfoq et al. 2022). Such an approach is simple and strong but likely sub-optimal when the features are required to be personalized. We agree on the concept of learning powerful representation but relax the single-model constraint by maintaining multiple shareable basis models. Another related topic *federated domain generalization* (Nguyen, Torr, and Lim 2022; Zhang et al. 2023) aims to learn a model that will be generalized to new domains, but not for personalization.

Personalized layers. Given a global model, which layers/components in a network should be personalized to tailor to local distributions attracts increasing attention lately (Shen, Zhou, and Yu 2022; Liang et al. 2020; Li et al. 2021b; Bui et al. 2019; Arivazhagan et al. 2019). Our goal is orthogonal to this direction since we focus on summarizing participating clients for new clients. For simplicity, we consider all the layers adaptable. Incorporating these techniques to select a partial network to improve further will be our future work.

Meta-learning. The most relevant approach to ours is meta-learning, which learns a meta-model for rapid personalization for (new) clients (Khodak, Balcan, and Talwalkar 2019; Chen et al. 2018; Fallah, Mokhtari, and Ozdaglar 2020; Jiang et al. 2019). However, it requires splitting/reusing the training data for meta-validation. Besides, it typically fine-tunes the entire meta-model for each client. Both are not favorable in low data regimes. Other methods model the relationships between clients (Zhang et al. 2021c; Huang et al. 2021) for initialization or regularization. The closest work to ours is (Shamsian et al. 2021) that summarizes local models into a HyperNetwork (Ha, Dai, and Le 2017). We provide a more detailed comparison in Sec. 4.2.

Lastly, **FEDBASIS** is inspired by 1) *architecture designs in centralized learning that improve a single neural network* (Yang et al. 2019; Chen et al. 2020; Zhang et al. 2021b) and 2) the concept of formulating task models as model linear combinations (Evgeniou and Pontil 2007). Our novelty is in

extending such a concept to PFL through more effective and scalable implementation, identifying difficulties in optimization, and resolving them accordingly.

3 Preliminary

We first provide a short background. In federated learning (FL), the training data are separately collected and stored by M clients. Each client $m \in [M]$ keeps a private set $\mathcal{D}_m = \{(\mathbf{x}_i, y_i)\}_{i=1}^{|\mathcal{D}_m|}$, where \mathbf{x} is the input (e.g., images) and $y \in \{1, \dots, C\} = [C]$ is the true label.

Given the loss function ℓ (e.g., cross-entropy) and the empirical risk $\mathcal{L}_m(\boldsymbol{\theta}) = \frac{1}{|\mathcal{D}_m|} \sum_{(\mathbf{x}_i, y_i) \in \mathcal{D}_m} \ell(y_i, h_{\boldsymbol{\theta}}(\mathbf{x}_i))$ of client m , where $h_{\boldsymbol{\theta}}$ denotes a model parameterized by $\boldsymbol{\theta}$, **personalized federated learning (PFL)** aims to learn for each client m a personalized model $\boldsymbol{\theta}_m$ tailored to client m 's data distribution. While there is no agreed objective function, many existing works (Smith et al. 2017; Li et al. 2021a; Dinh, Tran, and Nguyen 2020; Hanzely et al. 2020; Hanzely and Richtárik 2020; Li and Wang 2019) solve an optimization problem similar to

$$\min_{\{\boldsymbol{\Omega}, \boldsymbol{\theta}_1, \dots, \boldsymbol{\theta}_M\}} \frac{1}{M} \sum_{m=1}^M \mathcal{L}_m(\boldsymbol{\theta}_m) + \mathcal{R}(\boldsymbol{\Omega}, \boldsymbol{\theta}_1, \dots, \boldsymbol{\theta}_M), \quad (1)$$

where \mathcal{R} is a regularizer to overcome overfitting and $\boldsymbol{\Omega}$ is its learnable parameter.

Since the training data are decentralized, Eq. (1) is typically solved iteratively between local training at the clients and global aggregation at the server (for $\boldsymbol{\Omega}$) for multiple rounds, inspired by FEDAVG (McMahan et al. 2017).

Challenges in encompassing new clients. Although solving Eq. (1) can obtain personalized models, it relies on every client to participate in the training. *In reality, not all clients can join the federated training process due to communication or time constraints*, and it remains unclear how to deal with new client $m' \notin [M]$ who arrives *after the federated training is finished*. While fine-tuning a pre-trained global model with new client's data can produce a personalized model, it is prone to over-fitting (Li et al. 2021a; Pillutla et al. 2022; Wu et al. 2022; Fallah, Mokhtari, and Ozdaglar 2020) even with regularization (as will be verified in Sec. 6.2). Also, it does not fully leverage the relationships of participating clients, as discussed in Sec. 1.

4 FEDBASIS: PFL with Shareable Bases

To resolve these issues, we propose a novel personalization approach inspired by (Changpinyo et al. 2016; Evgeniou and Pontil 2007). We start with the assumption and formulation, followed by theoretical motivation and implementation.

4.1 Formulation

Assumption. For both participating clients and new clients, the clients' local data share similarity (e.g., domains, styles, classes, etc) — a common assumption made in multi-task learning (Evgeniou and Pontil 2007). It is likely that we can use a much smaller set of models $\{\mathbf{v}_1, \dots, \mathbf{v}_K\}$, $K \ll M$, $|\mathbf{v}| = |\boldsymbol{\theta}|$, to construct high-quality personalized models.

Shareable bases. We represent each personalized model's parameters (i.e., weights) $\boldsymbol{\theta}_m$ by a small set of K *basis* models $\mathcal{V} = \{\mathbf{v}_1, \dots, \mathbf{v}_K\}$ shared among clients

$$\boldsymbol{\theta}_m = \boldsymbol{\theta}(\boldsymbol{\alpha}_m, \mathcal{V}) = \sum_k \boldsymbol{\alpha}_m[k] \times \mathbf{v}_k, \quad (2)$$

where $\boldsymbol{\alpha}_m \in \Delta^{K-1}$ is a K -dimensional vector on the $(K-1)$ -simplex, seen as the personalized convex combination coefficients. That is, each personalized model is a convex combination of the basis models. We note that such a combination operation is linear only *within each neural network layer*; the synthesized model is still a neural network with non-linear operations. The representative ability thus remains versatile for constructing personalized models.

Objective function. Building upon the model representation in Eq. (2) and the optimization problem in Eq. (1), we define our FEDBASIS PFL problem for learning both the bases $\mathcal{V} = \{\mathbf{v}_1, \dots, \mathbf{v}_K\}$ and the coefficients $\mathcal{A} = \{\boldsymbol{\alpha}_1, \dots, \boldsymbol{\alpha}_M\}$ as²

$$\begin{aligned} \min_{\mathcal{A}=\{\boldsymbol{\alpha}_m\}_{m=1}^M, \mathcal{V}=\{\mathbf{v}_k\}_{k=1}^K} \quad & \frac{1}{M} \sum_{m=1}^M \mathcal{L}_m(\boldsymbol{\theta}_m), \\ \text{where } \boldsymbol{\theta}_m = \sum_k \boldsymbol{\alpha}_m[k] \times \mathbf{v}_k. \end{aligned} \quad (3)$$

Training. We solve Eq. (3) in a federated setting in Sec. 4.3.

Personalization for new clients. To generate the personalized model, a new client m' receives the learned \mathcal{V} and finds its specific combination coefficients $\boldsymbol{\alpha}_{m'}$ by SGD with its local data while keeping \mathcal{V} frozen, i.e., $\boldsymbol{\alpha}_{m'} = \arg \min_{\boldsymbol{\alpha}} \mathcal{L}_{m'}(\boldsymbol{\theta}(\boldsymbol{\alpha}, \mathcal{V}))$ based on Eq. (2). Since $|\boldsymbol{\alpha}_{m'}|$ is mere K per client, it can be robustly learned with fewer data.

Remark. We introduce additional advantages of FEDBASIS. First, in inference, FEDBASIS enjoys the same memory footprint and computation cost as a single basis model. Convexly combining the parameters (not the predictions!) of the basis models in \mathcal{V} layer-by-layer according to $\boldsymbol{\alpha}_{m'}$ will merge them into a single personalized model $\boldsymbol{\theta}_{m'}$. The inference cost thus remains constant, not scaling with K .

Second, compared to PFL methods based on meta-learning (Fallah, Mokhtari, and Ozdaglar 2020; Finn, Abbeel, and Levine 2017), which fine-tune the entire or partial model for each (new) client from the meta-learned initialization, we combine the bases *shared* by all clients into a personalized model by learning only a small coefficient vector. This makes FEDBASIS more robust to overfitting and hyperparameters when the new client's local data size is small. We will discuss the theoretical benefits of this personalization formulation next in Sec. 4.2.

4.2 Theoretical Motivation

The theoretical benefit of *summarizing* the clients with fewer *trainable* parameters is outlined by Theorem 1 in (Shamsian et al. 2021), which investigates learning a low-rank approximation over all the personalized model's parameters to

²We drop the regularization term in Eq. (1) as the convex combination itself is a form of regularization (Evgeniou and Pontil 2007). We implement $\boldsymbol{\alpha}$ by a softmax function in our experiments.

reconstruct them. Namely, each personalized model can be represented similarly as in Eq. (2); the theoretical analysis can therefore be applied to FEBASIS. In the following, we briefly review the analysis in the context of Sec. 4.1. The assumptions follow Sec. 4.5 in (Shamsian et al. 2021).

Let $\mathcal{V} \in \mathbb{R}^{|\theta| \times K}$ be the dictionary matrix of total size Q , $\mathcal{A} = [\alpha_1, \dots, \alpha_M] \in \mathbb{R}^{K \times M}$ be the coefficient matrix, and L be the sum of their Lipschitz constants. That is, each client m learns an embedding vector $\alpha_m \in \mathbb{R}^K$ and there are M clients in total. There exists a sample size

$$N = \mathcal{O}\left(\frac{K}{\epsilon^2} \log \frac{L}{\delta} + \frac{Q}{M\epsilon^2} \log \frac{L}{\delta}\right) \quad (4)$$

such that if the training samples per client $|\mathcal{D}_m| > N$, the generalization gap between the true loss and the empirical risk of the personalized model $\theta_m := \theta(\alpha_m, \mathcal{V})$ will be bounded (i.e., $|\tilde{\mathcal{L}}_m(\theta_m) - \mathcal{L}_m(\theta_m)| \leq \epsilon$) with probability at least $1 - \delta$, for all clients. The second term in Eq. (4) implies that summarizing many clients (a large M) with a small dictionary ($Q = |\theta| \times K$ with a small $K \ll M$) can notably improve generalization.

Remark. In (Shamsian et al. 2021), building on the analysis, the authors proposed to implement $\theta_m = \theta(\alpha_m, \mathcal{V})$ via a multi-layer perception (MLP), with α_m as the input and \mathcal{V} as the MLP’s parameters. In other words, they learned an MLP to predict a neural network θ_m , aka a hypernetwork (Ha, Dai, and Le 2017). This notoriously increases the size of \mathcal{V} (i.e., Q), making it hard to scale to deeper modern networks. Indeed, in (Shamsian et al. 2021), Q is about $100 \times |\theta|$ for handling $10 \sim 100$ clients, which is larger than the sum of clients’ model sizes. In contrast, our model representation in Eq. (2) exactly follows the formulation in the analysis. FEBASIS thus enjoys much fewer parameters — $Q = K \times |\theta|$ with a small K (4 to 8 in our experiments). Last but not least, (Shamsian et al. 2021) first learns θ_m and then learns α_m and \mathcal{V} to reconstruct it. The reconstructed model thus does not necessarily minimize the empirical risk. In contrast, we directly learn the bases and combination coefficients to construct personalized models that minimize the empirical risks, potentially leading to better personalization.

4.3 Federated Learning Algorithm

Since Eq. (3) cannot be solved directly, we present an FL algorithm to learn the basis models \mathcal{V} and the coefficients \mathcal{A} . To begin with, we introduce a baseline algorithm via the FEDAVG pipeline, iterating between local and global updates:

$$\text{Local: } \{\alpha_m^{(t)}, \tilde{\mathcal{V}}_m^{(t)}\} = \arg \min_{\{\alpha, \mathcal{V}\}} \mathcal{L}_m(\alpha, \mathcal{V}), \quad (5)$$

initialized by $\alpha = \frac{\mathbf{1}}{K}$ and $\mathcal{V} = \bar{\mathcal{V}}^{(t-1)}$,

$$\text{Global: } \bar{\mathcal{V}}^{(t)} \leftarrow \frac{1}{M} \sum_{m=1}^M \tilde{\mathcal{V}}_m^{(t)}, \quad (6)$$

where $\mathbf{1}$ is an all-one vector; we use $\mathcal{L}_m(\alpha, \mathcal{V})$ as a concise notation for $\mathcal{L}_m(\theta = \sum_k \alpha[k] \times \mathbf{v}_k)$. In each round t , a client first receives the latest K bases $\bar{\mathcal{V}}^{(t-1)}$ from the

server and updates the bases and the coefficient vector³ by minimizing the local loss \mathcal{L}_m . This results in a local copy of bases $\tilde{\mathcal{V}}_m^{(t)}$ for client m . The global aggregation then returns these M copies of bases to one copy $\bar{\mathcal{V}}^{(t)}$ by weight averaging (McMahan et al. 2017): the average is taken over the M local copies of each basis.

Problem of bases collapse. Unfortunately, such naive training can hardly outperform using a single basis, i.e., reducing to a single global model for all clients. To understand this, we investigate the federated training dynamics using a preliminary experiment on the PACS image classification dataset (Li et al. 2017) with ResNet18 (He et al. 2016), $K = 4$ bases, $M = 40$, and local epochs = 5. More details are in the supplementary. We check (1) the average pairwise cosine similarity between the basis model parameters; (2) the average entropy of the learned combination vectors. High entropy implies a more uniform combination vector.

In Fig. 2, we found that both the pairwise similarity and the entropy increase along with local training SGD iterations and training rounds. In other words, the bases gradually *collapse* to similar parameter values; the combination vectors of all clients nearly collapse to uniform combinations. Consequently, each basis model does not learn specialized knowledge; the whole bases \mathcal{V} basically degenerate to a single model (or K very similar models). By taking a deeper look at Fig. 2, we found that the collapse problem happens primarily within each local training round. To explain it, let us analyze the gradients derived at local training in Eq. (5),

$$\begin{aligned} \nabla_{\mathbf{v}_k} \mathcal{L}_m(\alpha, \mathcal{V}) &= \alpha[k] \times \nabla_{\theta} \mathcal{L}_m(\theta), \\ \nabla_{\alpha[k]} \mathcal{L}_m(\alpha, \mathcal{V}) &= \mathbf{v}_k \cdot \nabla_{\theta} \mathcal{L}_m(\theta). \end{aligned} \quad (7)$$

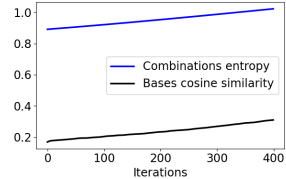
Interestingly, while with different magnitudes $\alpha[k]$, we see that $\nabla_{\mathbf{v}_k} \mathcal{L}_m(\alpha, \mathcal{V})$ pushes every local basis model $\mathbf{v}_k \in \tilde{\mathcal{V}}_m^{(t)}$ away from the same direction (since $\alpha[k] \geq 0$). As local basis models become similar towards $-\nabla_{\theta} \mathcal{L}_m(\theta)$, their inner products with $-\nabla_{\theta} \mathcal{L}_m(\theta)$ will get larger (i.e., positive) and similar, which would, in turn, push $\alpha[k]$ to be larger via a similar strength. In other words, the more SGD updates we perform within each round of local training, the more similar the local basis models will be and the more uniform the combination coefficients will be. *We propose the following treatments to prevent the collapse problem.*

Coordinate descent for the combination coefficients and bases. Based on the analysis, to prevent the collapse problem, α and \mathcal{V} should not be updated at the same time. We propose to first update α while freezing \mathcal{V} and then update \mathcal{V} while freezing α , each for multiple SGD steps, within every local training round. We note that at the beginning of each round of local training, $\mathbf{v}_k \cdot \nabla_{\theta} \mathcal{L}_m(\theta)$ is not necessarily negative. Updating α with frozen \mathcal{V} thus could potentially enlarge the difference among elements in α : forcing the personalized model to attend to a subset of bases.

Sharpening combination coefficients. Since $\alpha[k] \geq 0$, updating \mathbf{v}_k locally with $\nabla_{\mathbf{v}_k} \mathcal{L}_m(\alpha, \mathcal{V})$ would inevitably in-

³We note that client m only sees and updates its own combinations $\alpha_m^{(t)}$, not others’. $\alpha_m^{(t)}$ is initialized every round locally and we do not keep it stateful or share it with the server.

Within one-round local training



Along training rounds

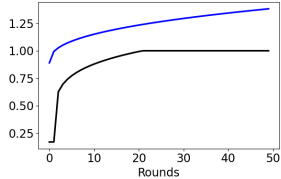


Figure 2: **Cosine similarity between bases, and the entropy of clients’ combination vectors on PACS dataset.** FEDBASIS by baseline training collapses to non-specialized bases and uniform combinations: (left) within one round of local training for one client; (right) along training rounds, where bases are aggregated at the server and the combinations entropy is averaged over clients.

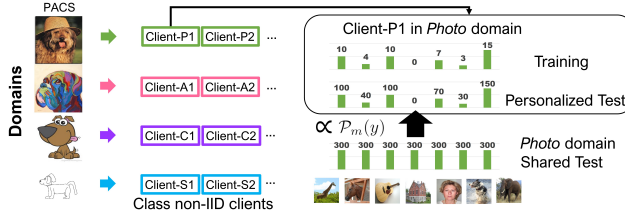


Figure 3: Example of our PFLBED construction for PFL.

crease the cosine similarity between basis models. The exception is when some bases get 0 gradients, i.e., $\alpha[k] = 0$. We therefore propose to *artificially* and *temporally* enforce this while calculating $\nabla_{v_k} \mathcal{L}_m(\alpha, \mathcal{V})$. We implement α by learning $\psi \in \mathbb{R}^K$ and reparameterizing it via a softmax function sharpened with a temperature $0 < \tau \leq 1$ as $\alpha[k] = \frac{\exp(\psi[k]/\tau)}{\sum_{k'} \exp(\psi[k']/\tau)}$.

Improved training algorithm. Putting these treatments together, we present an improved training algorithm for FEDBASIS based on Eq. (5). Please see the algorithms in the supplementary for the pseudo-code for multi-round training.

$$\begin{aligned}
 \text{Local: } & \text{ initialized by } \alpha = \frac{1}{K} \text{ and } \mathcal{V} = \bar{\mathcal{V}}^{(t-1)}, \quad [\text{Step 1}] \\
 & \alpha_m^{(t)} = \arg \min_{\alpha} \mathcal{L}_m(\alpha, \mathcal{V}), \quad [\text{Step 2}] \\
 & \alpha_m^{(t)\dagger} \leftarrow \text{SHARPEN}(\alpha_m^{(t)}; \tau), \quad [\text{Step 3}] \\
 & \tilde{\mathcal{V}}_m^{(t)} = \arg \min_{\mathcal{V}} \mathcal{L}_m(\alpha_m^{(t)\dagger}, \mathcal{V}), \quad [\text{Step 4}] \\
 \text{Global: } & \bar{\mathcal{V}}^{(t)} \leftarrow \frac{1}{M} \sum_{m=1}^M \tilde{\mathcal{V}}_m^{(t)}. \quad (8)
 \end{aligned}$$

Technical details. We provide implementation details, including how to initialize each basis in the supplementary.

Computation and communication cost. While FEDBASIS requires more cost in training K models, K is reasonably small and affordable for the modern Internet/GPUs.

5 PFLBED: bases for PFL Benchmarks

Many existing efforts are on building *generic* FL datasets (Hsu, Qi, and Brown 2020; Reddi et al. 2021), including the LEAF benchmarks (Caldas et al. 2018) but not for the PFL literature. For the sake of algorithm development, how should we construct a reliable evaluation? As side contributions, we propose the following aspects:

Table 1: Summary of the datasets and setups.

Dataset	Size	#Class	Resolution	Domain	Client Split
PACS	9K	7	224 ²	Styles	PFLBED
Office-Home	16K	65	224 ²	Styles	PFLBED
GLD23K	23K	203	224 ²	Natural	User ID
CIFAR-10/100	60K	10/100	32 ²	None	Dirichlet

➤ **Reliable evaluation.** We identify *two challenges* for realistic PFL evaluation on clients each with a small data size. First, *the test sets should be sufficiently large* for statistical reliability. Many previous works (Li et al. 2021a; Shamsian et al. 2021; Dinh, Tran, and Nguyen 2020) split an even smaller test set for each client. Second, the small local data size can lead to an even more problematic evaluation for realistic non-IID PFL since the *training/test distributions might be mismatched*. For example, the FEMNIST dataset in LEAF benchmark (Caldas et al. 2018) on average only has 226 images over 62 classes for each writer; many classes only have ≤ 1 images. It is unfaithful to split each client into train/test sets due to mismatches on label distributions $\mathcal{P}_m(y)$. Indeed, we found a large discrepancy $\frac{1}{M} \sum_m \|\mathcal{P}_m^{train}(y) - \mathcal{P}_m^{test}(y)\|_1 = 0.77$ even with a 50/50% split. See an illustration in the supplementary.

➤ **Cross-domain with non-IID $\mathcal{P}_m(x, y)$.** A realistic personalized dataset should have the joint distribution $\mathcal{P}_m(x, y)$ differ from client to client, not just $\mathcal{P}_m(x)$ (e.g., domains (Li et al. 2021b)) or $\mathcal{P}_m(y)$ (i.e., class labels (Collins et al. 2021; Fallah, Mokhtari, and Ozdaglar 2020; Shamsian et al. 2021)). Both the training data sizes and the class distributions should be skewed among clients to simulate realistic cases.

To achieve these desired properties for PFL training and evaluation, we propose to transform a cross-domain dataset \mathcal{D} that each input is associated with a domain annotation, into clients’ sets $\{(\mathcal{D}_m^{train}, \mathcal{D}_m^{test/val})\}$ with the following procedures, as illustrated in Fig. 3:

1. Separate \mathcal{D} based on its domain annotations.
2. For each domain, split the class-balanced test and validation sets which will later be shared with all clients from this domain. Take the rest as the training set.
3. For the training set per domain, create a class-heterogeneous partition, e.g., by the commonly used Dirichlet sampling (Hsu, Qi, and Brown 2019) for M' clients. Each client’s images are class-non-IID and from a single domain.
4. For each client m , record the class distributions $\mathcal{P}_m(y)$ of its training set.
5. For each client in each domain, assign the whole test set of the same domain as $\mathcal{D}_m^{test/val}$.
6. Compute $\frac{1}{M} \sum_m \frac{\sum_i \mathcal{P}_m(y_i) \mathbf{1}(y_i = \hat{y}_i)}{\sum_i \mathcal{P}_m(y_i)}$ as the client-wise average personalized accuracy during evaluation.

Evaluation on new clients. To evaluate how practical a personalized system can serve new clients, one can split the clients into participating/new clients groups and train on the participating group. After training, personalization is performed on each new client’s training set \mathcal{D}_m^{train} , and follows the same testing protocol.

Examples. We consider the two image object recognition datasets PACS (Li et al. 2017) and Office-Home (Venkateswara et al. 2017) that are widely used in domain adaptation, both providing 4 domain annotations of image *styles*. Following the proposed PFLBED procedures, we first split the samples of each domain into 60/20/5/15% for training, new, validation, and test sets. The training/new sets are further split for 20/10 of participating/new clients per domain by class non-IID sampling with $\text{Dirichlet}(0.3)$, following (Hsu, Qi, and Brown 2019).

6 Experiments

6.1 Settings (see the supplementary for details)

Dataset. Besides PFLBED, for completeness, we include a naturally non-IID Google Landmark (GLD-v2) (Weyand et al. 2020) dataset that has 233 photographers as clients (Hsu, Qi, and Brown 2020). We also consider standard PFL setups using CIFAR datasets (Krizhevsky, Hinton et al. 2009) (see Sec. 6.3). Tab. 1 summarizes the statistics.

Baselines. We compare FEBASIS to the state-of-the-art approaches discussed in Sec. 2. (1) *Personalized layers* finetunes only classifiers (FEDREP (Collins et al. 2021)) or batchnorm parameters (FEDBN (Li et al. 2021b)) for new clients. The most relevant approach to ours summarizes clients into a (2) *meta-model*, including PFEDHN (Shamsian et al. 2021) based on hypernetworks that generate a model for each client by learning an input embedding for the hypernetwork. Another method PER-FEDAVG (Fallah, Mokhtari, and Ozdaglar 2020)⁴ is based on MAML that learns a good initial model for fine-tuning. As pointed out by (Yu, Bagdasaryan, and Shmatikov 2020; Wang et al. 2019; Chen and Chao 2022; Cheng, Chadha, and Duchi 2021), fine-tuning (FT) on (3) *general representations* from global model like FEDAVG (McMahan et al. 2017) serves as a strong baseline. KNN-PER (Marfoq et al. 2022) further builds k -nearest neighbors classifier on top of the features locally.

FEBASIS. We train with 5 local epochs for both α and \mathcal{V} as described in Sec. 4.3, where $\tau = 0.1$ for sharpening the combinations and each ResNet block uses its own combination vector. The number of bases is 4/4/8 for PACS/Office-Home/GLD. For personalization, only the combinations and classifier are trained with \mathcal{V} frozen.

FL Training. ImageNet pre-trained ResNet-18 (He et al. 2016) with standard pre-processing is used with SGD optimizer with 0.9 momentum, 1e-4 weight decay, and 0.01 local learning rate. PFLBED/GLD datasets are trained for 100/200 rounds with 16/64 batch sizes and 5 local epochs (sample 100/10% participated clients) in each round.

Personalization. “New clients” are adapted with different local data sizes (Small/Moderate/Large) with the learning rate tuned from $\{0.005, 0.01, 0.05\}$ and 1e-4 weight decay.

⁴We focus on the better first-order version and we have compared it with the Hessian-free version in the supplementary.

6.2 Main Results

We highlight the following observations in Tab. 2:

- **Meta models are promising.** The best baseline is PER-FEDAVG+FT, supporting that modeling personalization from a meta-view is promising since it considers the inter-client relationships. Our FEBASIS summarizes bases over clients but with fewer trainable parameters per client, thus leading to more robust personalization and outperforming the baselines, especially on harder datasets Office-Home and GLD, supporting our Sec. 4.2.
- **Fine-tuning the feature extractor helps.** Fine-tuning on general features (e.g., FEDAVG’s global model) helps the performance, validating that the features are preferred to be client-specific. FEDAVG+FT is competitive against more recent methods like FEDREP and KNN-PER⁵.
- **Fine-tuning can be vulnerable w/o careful validation.** However, fine-tuning can be unstable w.r.t. the tuned epochs or likely suffer from overfitting (up to 7% of $|\Delta|$), especially when the local size is small. Note that, selecting the *best* epoch is not always feasible since the clients may not have enough data for validation (Wu et al. 2022); thus such robustness is important in practice.
- **FEBASIS is both robust and accurate.** FEBASIS can personalize the whole model by the layer composition ability enforced in training while being robust since it learns much fewer parameters per client. To see it from another view, we further compare the best baseline PER-FEDAVG+FT with different learning rates. In Fig. 4 (a), we observe FEBASIS is clearly more robust to hyperparameters such as the learning rates and stopping epoch.
- **Regularized personalization is not enough.** One might wonder if adding a regularizer to fine-tuning can help. We compare a regularizer-based method PFEDME (Dinh, Tran, and Nguyen 2020) and apply its Eq. (2) for PER-FEDAVG. As Tab. 3 shows, better regularizers can improve slightly but FEBASIS still outperforms.

6.3 Further Discussions

Visualization. To understand FEBASIS, we visualize the learned combinations in Fig. 4 (b). Interestingly, we see the clients group together according to domains especially in the latter blocks (e.g., Office-Home Block 3 & 4). FEBASIS enables the shareable bases to automatically determine the collaboration among the non-IID clients.

Ablations. The ablation study (w/ moderate local size) in Tab. 4 verifies our designs in Sec. 4.

Sanity checks: conventional PFL setups on CIFAR. So far the main study is on our PFLBED setups, we provide two sets of standard PFL experiments on the CIFAR-10/100 benchmarks⁶ for proving the generalizability of FEBASIS. We use 3 bases for CIFAR experiments.

⁵Interestingly, KNN-PER seems to be less effective in such low-data regimes, consistent with (Marfoq et al. 2022). We were able to reproduce the original results where each client has more samples.

⁶Compared to PFLBED in Sec. 5, these simulated datasets are single-domain and purely class non-IID. The evaluation is faithful since the training/test sets are distributionally matched.

Table 2: Personalized test accuracy (%) on non-IID new clients. Averaged over 3 runs. Variances and more results are provided in the supplementary. Each method personalizes on each client’s local data of different sizes. We personalize by fine-tuning (FT) for 20 epochs and record at the **Last** and **Best** (by validation) epoch, and measure the difference $|\Delta|$ as personalization robustness.

Dataset (Part./New Clients)		PACS (80/40)				Office-Home (80/40)				GLD23k (117/116)			
Local Size for Personalization		S	M	S	M	S	M	S	M	L			
Approach / Stopping Epoch		Last	Best	$ \Delta $	Last	Best	$ \Delta $	Last	Best	$ \Delta $	Last	Best	$ \Delta $
Personalized Layers	FEDREP	87.4	87.4	0.0	92.5	92.4	0.1	75.6	75.6	0.0	76.0	76.1	0.1
	FEDBN	86.2	88.2	2.0	92.4	92.4	0.0	76.9	77.0	0.1	78.1	78.1	0.0
Meta-Model	PFEDHN	85.4	-	85.5	-	74.1	-	74.3	-	74.5	-	75.6	-
	PFEDHN+FT	90.5	91.2	0.7	90.4	91.4	1.0	76.2	77.2	1.0	77.1	77.6	0.5
	PER-FEDAVG+FT	95.4	95.6	0.2	96.2	96.3	0.1	84.3	84.4	0.1	86.1	86.2	0.1
General Representation	KNN-PER	71.6	-	71.6	-	50.4	-	54.5	-	54.0	-	57.4	-
	KNN-PER+FT	72.7	72.7	0.0	79.4	79.7	0.3	51.6	52.4	0.8	54.2	54.4	0.2
	FEDAVG	88.1	-	88.1	-	73.1	-	73.1	-	45.4	-	45.4	-
	FEDAVG+FT	86.1	91.9	5.8	90.5	90.5	0.0	76.1	77.4	1.3	78.2	78.5	0.3
Ours	FEBASIS	95.2	95.2	0.0	96.2	96.2	0.0	87.4	87.5	0.1	87.5	87.7	0.2

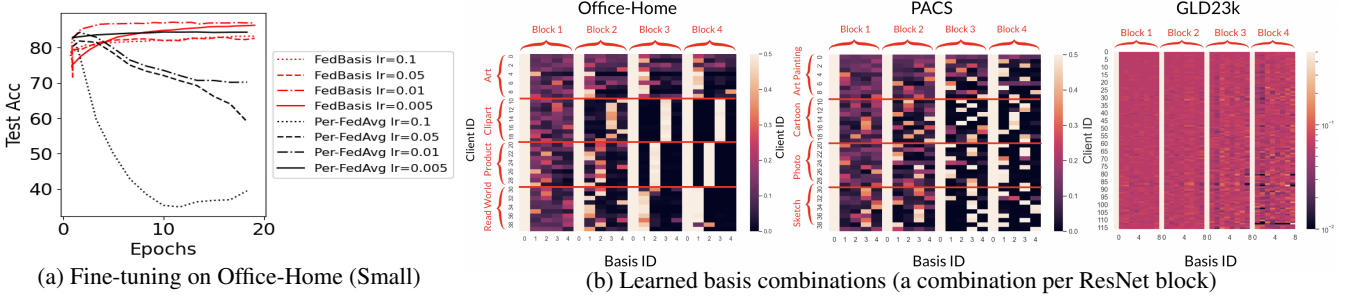


Figure 4: (a) **FEBASIS** for more robust personalization. Fine-tuning curves with different learning rates. (b) **Visualization of $\{\alpha_m\}$** .

Table 3: Office-Home new clients regularized fine-tuning (FT).

FL Training	FT Regularizer	Acc.
PER-FEDAVG	Weight decay / Eq. (2) in PFEDME	84.3 / 84.5
PFEDME	Weight decay / Eq. (2) in PFEDME	77.5 / 77.8
FEBASIS	Weight decay	87.5

Table 4: Ablation studies of FEBASIS designs in Sec. 4.

CoordinateDescent	τ	Office-Home Acc.
	0.1	83.5
	1.0	87.1
	0.1	87.5

First, we use the authors’ official codes to reproduce and compare Table 1 experiments in (Collins et al. 2021) of participating clients, including the backbone and training detail. Tab. 5 shows FEBASIS is also effective in this setup and performs comparably to the state of the arts like FEDREP based on global features. We note that this is expected since the images are single-domain thus the features might not have much room to be personalized. This can be seen in the saturated improvements that many PFL algorithms perform similarly to FEDAVG+FT in this class non-IID setting. In contrast, PFLBED in Sec. 5 is cross-domain and class non-IID where fine-tuning features is important.

Second, we further evaluate new client personalization as our main goal in Tab. 2. We follow Tab. 5 but now split the

Table 5: Test accuracy of *participating* clients on conventional PFL of CIFAR (100 clients, each has 5 classes). We reproduce the setting and the baseline results of Table 1 in (Collins et al. 2021).

Method	CIFAR10	CIFAR100
FedAvg (McMahan et al. 2017)/ +FT	51.8/73.7	23.9/79.3
FedProx (Li et al. 2020)/ +FT	51.0/72.8	20.2/78.5
(Karimireddy et al. 2020)/ +FT	47.3/68.2	20.3/78.9
Fed-MTL (Smith et al. 2017)	58.3	71.5
Per-FedAvg (Fallah et al. 2020)	67.2	72.1
LG-Fed (Liang et al. 2020)	63.0	72.4
L2GD (Hanzely and Richtárik 2020)	60.0	72.1
APFL (Deng, Kamani, and Mahdavi 2020)	72.2	78.2
Ditto (Li et al. 2021a)	70.3	78.9
FedPer (Arivazhagan et al. 2019)	73.8	76.0
FedRep (Collins et al. 2021)	75.7	79.1
FEBASIS	$ 75.5 \pm 0.7 $	80.8 ± 0.5

100 clients into 80/20 clients for training and evaluation. Each new client is fine-tuned for 10 epochs. In Tab. 6, we see our FEBASIS is competitive against the strongest baseline (PER-FEDAVG+FT).

7 Conclusion

We present a novel framework called FEBASIS for robust personalization of new clients. FEBASIS synthesizes personalized models using a few shareable basis models learned from participating clients in federated training. This reduces the learnable parameter size for each client for personaliza-

Table 6: CIFAR personalization on *new* clients. 80/20 participating /new clients, each has 5 classes.

Method	CIFAR10	CIFAR100
FEDAVG+FT	72.7 ± 0.3	78.1 ± 0.3
PER-FEDAVG+FT	74.8 ± 0.4	78.4 ± 0.4
FEDBASIS	76.5 ± 0.6	79.2 ± 0.4

tion and mitigates the vulnerability of fine-tuning. We design our federated algorithm to overcome the difficulty in optimization systematically. We also present a carefully designed benchmark PFLBED to support future research. We discuss limitations and future work in the supplementary.

Acknowledgments

This research is supported in part by grants from the National Science Foundation (IIS-2107077, OAC-2118240, and OAC-2112606) and Cisco Research. We are thankful for the generous support of the computational resources by the Ohio Supercomputer Center.

References

Achituve, I.; Shamsian, A.; Navon, A.; Chechik, G.; and Feitaya, E. 2021. Personalized Federated Learning with Gaussian Processes. *Advances in Neural Information Processing Systems*, 34: 8392–8406.

Arivazhagan, M. G.; Aggarwal, V.; Singh, A. K.; and Choudhary, S. 2019. Federated learning with personalization layers. *arXiv preprint arXiv:1912.00818*.

Bui, D.; Malik, K.; Goetz, J.; Liu, H.; Moon, S.; Kumar, A.; and Shin, K. G. 2019. Federated user representation learning. *arXiv preprint arXiv:1909.12535*.

Caldas, S.; Wu, P.; Li, T.; Konečný, J.; McMahan, H. B.; Smith, V.; and Talwalkar, A. 2018. Leaf: A benchmark for federated settings. *arXiv preprint arXiv:1812.01097*.

Changpinyo, S.; Chao, W.-L.; Gong, B.; and Sha, F. 2016. Synthesized classifiers for zero-shot learning. In *CVPR*.

Chen, F.; Luo, M.; Dong, Z.; Li, Z.; and He, X. 2018. Federated Meta-Learning with Fast Convergence and Efficient Communication. *arXiv: Learning*.

Chen, H.-Y.; and Chao, W.-L. 2022. On Bridging Generic and Personalized Federated Learning for Image Classification. In *International Conference on Learning Representations*.

Chen, Y.; Dai, X.; Liu, M.; Chen, D.; Yuan, L.; and Liu, Z. 2020. Dynamic Convolution: Attention Over Convolution Kernels. In *IEEE/CVF Conference on Computer Vision and Pattern Recognition (CVPR)*.

Cheng, G.; Chadha, K.; and Duchi, J. 2021. Fine-tuning is fine in federated learning. *arXiv preprint arXiv:2108.07313*.

Collins, L.; Hassani, H.; Mokhtari, A.; and Shakkottai, S. 2021. Exploiting Shared Representations for Personalized Federated Learning. In *ICML*.

Deng, Y.; Kamani, M. M.; and Mahdavi, M. 2020. Adaptive personalized federated learning. *arXiv preprint arXiv:2003.13461*.

Dinh, C. T.; Tran, N. H.; and Nguyen, T. D. 2020. Personalized federated learning with Moreau envelopes. In *NeurIPS*.

Evgeniou, A.; and Pontil, M. 2007. Multi-task feature learning. In *NeurIPS*.

Fallah, A.; Mokhtari, A.; and Ozdaglar, A. 2020. Personalized federated learning: A meta-learning approach. In *NeurIPS*.

Finn, C.; Abbeel, P.; and Levine, S. 2017. Model-agnostic meta-learning for fast adaptation of deep networks. In *International conference on machine learning*, 1126–1135. PMLR.

Ghosh, A.; Chung, J.; Yin, D.; and Ramchandran, K. 2020. An efficient framework for clustered federated learning. *Advances in Neural Information Processing Systems*, 33: 19586–19597.

Ha, D.; Dai, A.; and Le, Q. V. 2017. Hypernetworks. In *ICLR*.

Hanzely, F.; Hanzely, S.; Horváth, S.; and Richtárik, P. 2020. Lower bounds and optimal algorithms for personalized federated learning. In *NeurIPS*.

Hanzely, F.; and Richtárik, P. 2020. Federated learning of a mixture of global and local models. *arXiv preprint arXiv:2002.05516*.

He, K.; Zhang, X.; Ren, S.; and Sun, J. 2016. Deep residual learning for image recognition. In *CVPR*.

Hsu, T.-M. H.; Qi, H.; and Brown, M. 2019. Measuring the effects of non-identical data distribution for federated visual classification. *arXiv preprint arXiv:1909.06335*.

Hsu, T.-M. H.; Qi, H.; and Brown, M. 2020. Federated visual classification with real-world data distribution. In *European Conference on Computer Vision*, 76–92. Springer.

Huang, Y.; Chu, L.; Zhou, Z.; Wang, L.; Liu, J.; Pei, J.; and Zhang, Y. 2021. Personalized Cross-Silo Federated Learning on Non-IID Data. In *AAAI*.

Jiang, Y.; Konecný, J.; Rush, K.; and Kannan, S. 2019. Improving Federated Learning Personalization via Model Agnostic Meta Learning. *ArXiv*, abs/1909.12488.

Jordan, M. I.; and Mitchell, T. M. 2015. Machine learning: Trends, perspectives, and prospects. *Science*, 349(6245): 255–260.

Kairouz, P.; McMahan, H. B.; Avent, B.; Bellet, A.; Bennis, M.; Bhagoji, A. N.; Bonawitz, K.; Charles, Z.; Cormode, G.; Cummings, R.; et al. 2019. Advances and open problems in federated learning. *arXiv preprint arXiv:1912.04977*.

Karimireddy, S. P.; Kale, S.; Mohri, M.; Reddi, S.; Stich, S.; and Suresh, A. T. 2020. SCAFFOLD: Stochastic controlled averaging for federated learning. In *ICML*.

Khodak, M.; Balcan, M.-F.; and Talwalkar, A. 2019. Adaptive Gradient-Based Meta-Learning Methods. In *NeurIPS*.

Krizhevsky, A.; Hinton, G.; et al. 2009. Learning multiple layers of features from tiny images.

Li, D.; and Wang, J. 2019. FedMD: Heterogenous Federated Learning via Model Distillation. *arXiv preprint arXiv:1910.03581*.

Li, D.; Yang, Y.; Song, Y.-Z.; and Hospedales, T. M. 2017. Deeper, broader and artier domain generalization. In *Proceedings of the IEEE international conference on computer vision*, 5542–5550.

Li, T.; Hu, S.; Beirami, A.; and Smith, V. 2021a. Ditto: Fair and robust federated learning through personalization. In *International Conference on Machine Learning*, 6357–6368. PMLR.

Li, T.; Sahu, A. K.; Zaheer, M.; Sanjabi, M.; Talwalkar, A.; and Smith, V. 2020. Federated optimization in heterogeneous networks. In *MLSys*.

Li, X.; JIANG, M.; Zhang, X.; Kamp, M.; and Dou, Q. 2021b. Fed{BN}: Federated Learning on Non-{IID} Features via Local Batch Normalization. In *ICLR*.

Liang, P. P.; Liu, T.; Ziyin, L.; Salakhutdinov, R.; and Morency, L.-P. 2020. Think locally, act globally: Federated learning with local and global representations. *arXiv preprint arXiv:2001.01523*.

Luo, J.; and Wu, S. 2022. Adapt to adaptation: Learning personalization for cross-silo federated learning. In *IJCAI: proceedings of the conference*, volume 2022, 2166. NIH Public Access.

Mairal, J.; Bach, F.; Ponce, J.; and Sapiro, G. 2009. Online dictionary learning for sparse coding. In *ICML*, 689–696.

Marfoq, O.; Neglia, G.; Bellet, A.; Kameni, L.; and Vidal, R. 2021. Federated multi-task learning under a mixture of distributions. *Advances in Neural Information Processing Systems*, 34.

Marfoq, O.; Neglia, G.; Vidal, R.; and Kameni, L. 2022. Personalized Federated Learning through Local Memorization. In *International Conference on Machine Learning*, 15070–15092. PMLR.

McMahan, H. B.; Moore, E.; Ramage, D.; Hampson, S.; et al. 2017. Communication-efficient learning of deep networks from decentralized data. In *AISTATS*.

Nguyen, A. T.; Torr, P.; and Lim, S. N. 2022. Fedsr: A simple and effective domain generalization method for federated learning. *Advances in Neural Information Processing Systems*, 35: 38831–38843.

Papernot, N.; McDaniel, P.; Sinha, A.; and Wellman, M. 2016. Towards the science of security and privacy in machine learning. *arXiv preprint arXiv:1611.03814*.

Pillutla, K.; Malik, K.; Mohamed, A.-R.; Rabbat, M.; Sanjabi, M.; and Xiao, L. 2022. Federated learning with partial model personalization. In *International Conference on Machine Learning*, 17716–17758. PMLR.

Reddi, S.; Charles, Z.; Zaheer, M.; Garrett, Z.; Rush, K.; Konečný, J.; Kumar, S.; and McMahan, H. B. 2021. Adaptive Federated Optimization. In *ICLR*.

Reisser, M.; Louizos, C.; Gavves, E.; and Welling, M. 2021. Federated mixture of experts. *arXiv preprint arXiv:2107.06724*.

Ruan, Y.; and Joe-Wong, C. 2022. Fedsoft: Soft clustered federated learning with proximal local updating. In *Proceedings of the AAAI Conference on Artificial Intelligence*, volume 36, 8124–8131.

Rudovic, O.; Lee, J.; Dai, M.; Schuller, B.; and Picard, R. W. 2018. Personalized machine learning for robot perception of affect and engagement in autism therapy. *Science Robotics*, 3(19): eaao6760.

Shamsian, A.; Navon, A.; Fetaya, E.; and Chechik, G. 2021. Personalized Federated Learning using Hypernetworks. In *ICML*.

Shen, Y.; Zhou, Y.; and Yu, L. 2022. CD2-pFed: Cyclic Distillation-guided Channel Decoupling for Model Personalization in Federated Learning. In *Proceedings of the IEEE/CVF Conference on Computer Vision and Pattern Recognition*, 10041–10050.

Smith, V.; Chiang, C.-K.; Sanjabi, M.; and Talwalkar, A. S. 2017. Federated multi-task learning. In *NeurIPS*.

Sun, B.; Huo, H.; Yang, Y.; and Bai, B. 2021. Partialfed: Cross-domain personalized federated learning via partial initialization. *Advances in Neural Information Processing Systems*, 34: 23309–23320.

Tan, A. Z.; Yu, H.; Cui, L.; and Yang, Q. 2022. Towards personalized federated learning. *IEEE Transactions on Neural Networks and Learning Systems*.

Venkateswara, H.; Eusebio, J.; Chakraborty, S.; and Panchanathan, S. 2017. Deep hashing network for unsupervised domain adaptation. In *Proceedings of the IEEE conference on computer vision and pattern recognition*, 5018–5027.

Wang, K.; Mathews, R.; Kiddon, C.; Eichner, H.; Beaufays, F.; and Ramage, D. 2019. Federated Evaluation of On-device Personalization. *ArXiv*, abs/1910.10252.

Weyand, T.; Araujo, A.; Cao, B.; and Sim, J. 2020. Google landmarks dataset v2-a large-scale benchmark for instance-level recognition and retrieval. In *Proceedings of the IEEE/CVF conference on computer vision and pattern recognition*, 2575–2584.

Wu, S.; Li, T.; Charles, Z.; Xiao, Y.; Liu, Z.; Xu, Z.; and Smith, V. 2022. Motley: Benchmarking Heterogeneity and Personalization in Federated Learning. *arXiv preprint arXiv:2206.09262*.

Yang, B.; Bender, G.; Le, Q. V.; and Ngiam, J. 2019. Cond-conv: Conditionally parameterized convolutions for efficient inference. *Advances in Neural Information Processing Systems*, 32.

Yu, T.; Bagdasaryan, E.; and Shmatikov, V. 2020. Salvaging federated learning by local adaptation. *arXiv preprint arXiv:2002.04758*.

Zec, E. L.; Mogren, O.; Martinsson, J.; Sütfeld, L. R.; and Gillblad, D. 2020. Federated learning using a mixture of experts. *arXiv preprint arXiv:2010.02056*.

Zhang, J.; Guo, S.; Ma, X.; Wang, H.; Xu, W.; and Wu, F. 2021a. Parameterized Knowledge Transfer for Personalized Federated Learning. *Advances in Neural Information Processing Systems*, 34.

Zhang, M.; Chu, C.-T.; Zhmoginov, A.; Howard, A.; Jou, B.; Zhu, Y.; Zhang, L.; Hwa, R.; and Kovashka, A. 2021b. BasisNet: Two-stage Model Synthesis for Efficient Inference. In *Proceedings of the IEEE/CVF Conference on Computer Vision and Pattern Recognition*, 3081–3090.

Zhang, M.; Sapra, K.; Fidler, S.; Yeung, S.; and Alvarez, J. M. 2021c. Personalized Federated Learning with First Order Model Optimization. In *ICLR*.

Zhang, R.; Xu, Q.; Yao, J.; Zhang, Y.; Tian, Q.; and Wang, Y. 2023. Federated domain generalization with generalization adjustment. In *Proceedings of the IEEE/CVF Conference on Computer Vision and Pattern Recognition*, 3954–3963.

Supplementary Materials

We provide the details omitted in the main paper.

- Appendix A: pseudo codes and more discussion of FEBASIS (cf. Sec. 4 of the main paper).
- Appendix B: additional details of experiment setups (cf. Sec. 4 and Sec. 6 of the main paper).
- Appendix C: additional discussion on the datasets and PFLBED (cf. Sec. 5 of the main paper).
- Appendix D: additional results and discussion (cf. Sec. 4 and Sec. 6 of the main paper, including the bases collapse problem in Sec. 4.3).

A FEBASIS Algorithm

Algorithm 1: FEBASIS— federated training for the bases

Server input : initial global basis parameter $\bar{\mathcal{V}}$;
Client m 's input : local loss \mathcal{L}_m , temperature τ ;
1 **for** $t \leftarrow 1$ to T **rounds do**
2 **Communicate** $\bar{\mathcal{V}}$ to all clients $m \in [M]$;
3 **for** each client $m \in [M]$ **in parallel do**
4 **Initialize** $\{\alpha_m, \mathcal{V}\}$ by $\{\frac{1}{K}, \bar{\mathcal{V}}\}$;
5 $\alpha_m^* = \arg \min_{\alpha_m} \mathcal{L}_m(\alpha_m, \mathcal{V})$
6 $\alpha_m^{*\dagger} \leftarrow \text{SHARPEN}(\alpha_m^*; \tau)$;
7 $\mathcal{V}_m^* = \arg \min_{\mathcal{V}} \mathcal{L}_m(\alpha_m^{*\dagger}, \mathcal{V})$;
8 **Communicate** \mathcal{V}_m^* to the server;
9 **end**
10 **Construct** $\bar{\mathcal{V}} = \frac{1}{M} \sum_{m=1}^M \mathcal{V}_m^*$;
11 **end**
Server output : $\bar{\mathcal{V}}$;

Algorithm 2: FEBASIS— generate a personalized model

Client m 's input : initial global basis parameter \mathcal{V} , local loss \mathcal{L}_m ;
1 **Initialize** α_m by $\frac{1}{K}$;
2 $\alpha_m^* = \arg \min_{\alpha_m} \mathcal{L}_m(\alpha_m, \mathcal{V})$
3 **Construct** $\theta_m(\alpha_m, \mathcal{V}) = \sum_k \alpha_m[k] \times \mathbf{v}_k$;
Client m 's output: θ_m ;

We provide a summary in Algorithm 1 for training our FEBASIS (cf. Sec. 4.3 in the main paper) and Algorithm 2 shows how to use it for generating a personalized model. Similar to the FEDAVG algorithm, our FEBASIS also executes a multi-round training procedure between the local training at the clients and aggregation at the server.

The goal of FEBASIS is to collaboratively train K basis models $\mathcal{V} = \{\mathbf{v}_k\}_{k=1}^K$ which can be used to combine into personalized models based on each client's combination coefficient $\alpha_m \in \mathbb{R}^K$ (or more specifically, $\Delta^{(K-1)}$; see Eq. (2)) within limited T rounds of communications. The parameters are linearly combined layer by layer. Such specialized layers improve the performance with little extra inference cost. Our contribution is to extend such concepts to personalization in FL setting, identify optimization issues, and resolve them.

To effectively learn the bases for personalization, in Sec. 4.3, we introduce several important techniques in the local training to avoid bases collapse and encourage each basis to learn specialized knowledge. In each round of local training at a client m , it first initializes the bases \mathcal{V} using the one broadcast by the server. Next, we train α_m and \mathcal{V} with coordinate descent. We update α_m (for multiple SGD steps) while freezing \mathcal{V} (line 5 in Algorithm 1). To force the personalized model to attend to a subset of bases, we sharpen α_m by injecting a temperature into the Softmax function (line 6 in Algorithm 1). Then, we update \mathcal{V} (for multiple SGD steps) while freezing α_m . Finally, the updated bases are sent back to the server for a basis-wise average with other clients' updates.

The FEBASIS formulation enjoys several desired properties.

- The total learnable parameter size of all the personalized models (almost) does not scale with the number of clients. FEBASIS ultimately outputs the bases \mathcal{V} with combination coefficients α_m for each client m . Each client only has $|\alpha_m| = K$ personalized parameters, which is negligible compared to the model. After \mathcal{V} is trained, it can be used to generate personalized models for new clients. As discussed in Sec. 4.2, such formulation leads to more generalized personalization and robustness to small data sizes.
- For local training, the combined model only needs to be generated per mini-batch but not per instance, making it scalable to batch sizes.

- The size of communications is K times more but K is typically small ($4 \sim 8$ in our experiments).
- FEDBASIS does not increase clients’ computation cost in inference. After training, the basis models are combined into a single personalized model for each client. This is sharply different from approaches based on the mixture of models in that input needs to go through every expert and ensembles the predictions, where the cost is linear to the number of experts.

B More experimental details

B.1 Split new clients for evaluation

Following the proposed PFLBED procedures, we first split the samples of each domain into 60/20/5/15% for training, new, validation, and test sets. The training/new sets are further split for 20/10 of participating/new clients per domain by class non-IID sampling with Dirichlet(0.3), following (Hsu, Qi, and Brown 2019). In our experiments, to demonstrate the data efficiency of each of the methods, we consider different training sizes (**Small/Moderate/Large**) for personalization of each client. Concretely, for Office-Home and PACS, we use 50/100% of each client’s training set as the **S/M** setting for personalization, respectively. We note that, in PFLBED, we already split a relatively small set (20% of the overall data) and further split it into several new clients. On the other hand, for the GLD-v2 dataset, the clients are already split by User IDs, we thus randomly split 10/20/40% of each new client’s data as the training set and take the rest as the test/validation sets (we split 20% for validation).

B.2 Technical Extension

Block-wise combinations. In Eq. (2), it applies the same coefficient $\alpha_m[k]$ to combine the whole v_k into θ_m . Such a formula can be slightly relaxed to decouple the coefficients by layers, allowing it to learn different collaboration patterns. For instance, in our experiments on ResNets, we learn a coefficient vector for each of the 4 blocks and the classifier (instead for the whole network).

The major basis and warm-start for the bases. One concern is that an individual basis can be specialized but poorly generalized since it is likely trained on only partial data. We show this can be resolved easily with two tricks. First, we maintain a *major basis* that is always included in the combinations. That is, Eq. (2) becomes $\theta_m(\alpha_m, \mathcal{V}) = \frac{1}{2}(\mathbf{v}' + \sum_k \alpha_m[k] \times \mathbf{v}_k)$, where \mathbf{v}' is the major basis and the other bases personalize on top of it. Second, FEDBASIS can be a post-processing tool for a generic FL algorithm for personalizing new clients. Practically, we first run FEDAVG for a few rounds. The server collects the local models $\{\theta_m\}$, clusters them into K clusters, and initializes K basis models with the centroids. It warm-starts FEDBASIS since each basis already learns general knowledge and is somehow specialized. We run FEDAVG for 30% of the total rounds and collect its global/local models (Chen and Chao 2022) to warm-start the major/non-major bases, respectively.

B.3 Hyperparameters

For every method, we first conduct federated training, then personalize the trained model for further personalization on new clients as evaluation.

Training. We use an ImageNet pre-trained ResNet-18 (He et al. 2016) with standard ImageNet-style pre-processing, SGD optimizer with 0.9 momentum, 1e-4 weight decay, and 0.01 local learning rate. PFLBED/GLD datasets are trained for 100/200 rounds with 16/64 batch sizes and 5 local epochs for each participating client (sample 100/10%) in each round. All the methods including the baselines and ours use the same training process for a fair comparison. For FEDBASIS, it is trained with 5 local epochs for both α and \mathcal{V} as described in cf. Sec. 4.3 and Appendix B.2, where $\tau = 0.1$ for sharpening the combinations. The number of bases is 4/4/8 besides the major basis for PACS/Office-Home/GLD.

Evaluation. We consider that “new clients” are personalized with different local data sizes (**Small/Moderate/Large**) with the learning rate tuned from $\{0.005, 0.01, 0.05\}$ and 1e-4 weight decay. Each method is personalized in the way they proposed. We further consider different strategies including linear probes and fine-tuning and summarize in Tab. C for completeness.

Following the same personalization adaptation, each method is trained for each client to produce its personalized model. For the personalized layers approach, we first train by their algorithms, then personalize those layers for new clients like classifiers (FEDREP (Collins et al. 2021)) or batchnorm parameters (FEDBN (Li et al. 2021b)). KNN-PER (Marfoq et al. 2022) uses the global features of FEDAVG (McMahan et al. 2017) for k -nearest neighbors based classification locally. For PFEDHN (Shamsian et al. 2021), it first trains a hypernetwork that is a model generator. We follow (Shamsian et al. 2021) to train each client an input embedding for the hypernetwork to generate its personalized model (which can be further fine-tuned fully). PER-FEDAVG (Fallah, Mokhtari, and Ozdaglar 2020) is based on MAML that learns a good initial model for fine-tuning. Therefore, it should not be used directly. We consider using full fine-tuning on it. We focus on the better first-order version and we have compared it with the Hessian-free version in Tab. B. For personalization with FEDBASIS, only the combinations and classifier are trained.

C More details on the PFLBED dataset construction

C.1 Discussions on PFLBED

In Sec. 5, we provide several aspects including cross-domain and class non-IID $\mathcal{P}_m(\mathbf{x}, y)$, sufficient test samples, matched training/test splits, and distributional robustness evaluated with the class-balanced accuracy. We propose a standardized process

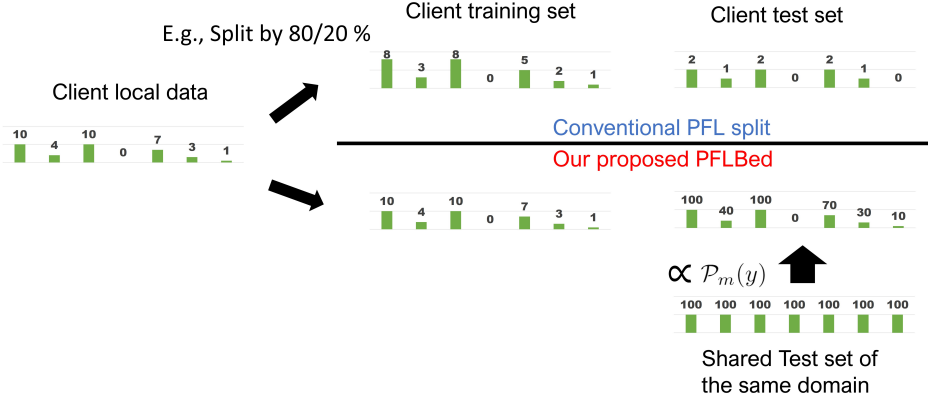


Figure A: Illustration of the difference between traditional PFL split and our proposed PFLBED in Sec. 5 for a client. For the conventional way, given that each client may have limited data per class, after a training/test split, the distribution might be no longer matched, leading to an unfaithful evaluation. On the contrary, Our proposed way uses a shared test set from the same domain and re-weight the examples in evaluation by classes (e.g., weighted accuracy).

called PFLBED to construct a faithful personalized dataset for PFL algorithm development. As examples, we propose to transform some existing datasets including PACS and Office-Home, that are widely used in bench-marking domain adaption tasks, into PFL datasets. These datasets are suitable for experimental use in research since they are created with clear domain differences such as image styles like *Photo* or *Art*. The illustration Fig. A shows the difference in preparing the test split for each client between the conventional PFL way and our proposed procedure based on PFLBED. For the conventional way, given that each client may have limited data per class, after a training/test split, the distribution might be no longer matched, leading to an unfaithful evaluation. On the contrary, Our proposed way uses a shared test set from the same domain and re-weight the examples in evaluation by classes (e.g., weighted accuracy). Currently, for the sake of simplicity, we consider each client comes from one domain so the test set can simply be all the test images from that domain. We note that it is straightforward to make each client from a mixture of domains.

In our experiments, for completeness, we also include the naturally partitioned dataset GLD-v2 (Weyand et al. 2020; Hsu, Qi, and Brown 2020), a dataset consisting of landmark photographs taken from various locations around the world by different photographers where each partition contains a photographer’s photos. We can view the style difference among the photographers as the domain gap thus treating each client as a domain.

C.2 Visualizations of PFLBED dataset client distribution

Here we show example client distributions of our proposed datasets for PFLBED. For PACS and Office-Home datasets, we follow the procedures outlined in Sec. 5 where each client is sampled from Dirichlet(0.3) within each domain. We visualize the distributions in Fig. B and Fig. C that the size of each point is proportional to the counts per class in a domain. Each column can be viewed as a single client’s label distribution. As we can see, our clients show both label space $\mathcal{P}_m(y)$ and domain space $\mathcal{P}_m(x)$ heterogeneity. In Appendix C.1 it shows the class distribution of the GLD dataset but it does not show domain differences through color differences since it is naturally non-IID without a specific domain annotation; each client can be directly treated as an independent domain.

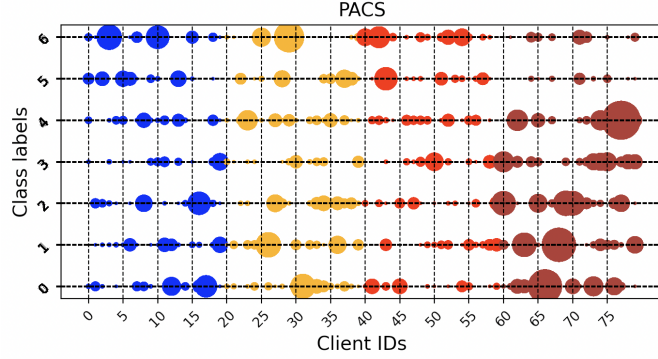


Figure B: Clients distribution of PACS dataset across 4 different domains. Each number on the horizontal axis represents a particular client for a total of $M = 80$ clients. Each number on the vertical axis represents a particular class label for a total of 7 classes. The maximum number of samples per class is 256.

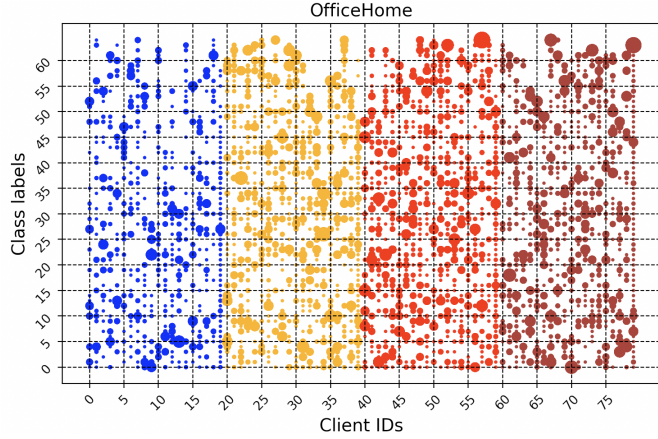


Figure C: Clients distribution of Office-Home dataset across 4 different domains. Each number on the horizontal axis represents a particular client for a total of $M = 80$ clients. Each number on the vertical axis represents a particular class label for a total of 65 classes. The maximum number of samples per class is 49.

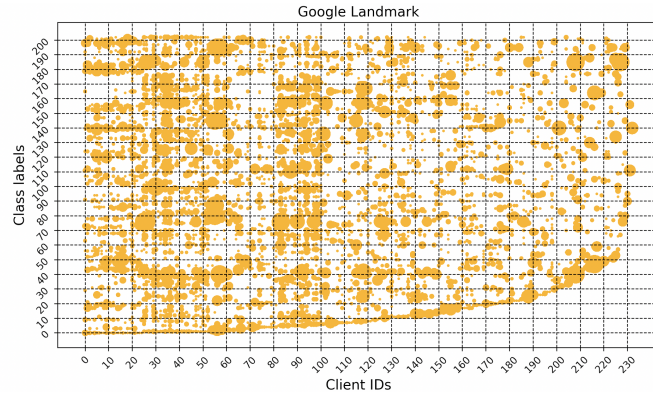


Figure D: Clients distribution of GLD23k dataset. Each number on the horizontal axis represents a particular client for a total of $M = 233$ clients. Each number on the vertical axis represents a particular class label for a total of $D = 203$ classes. The maximum number of samples per class is 100.

Table A: Baseline federated training algorithm for FEDBASIS on PACS datasets with different **communication frequencies**. We consider $M = 40$ participating clients and $K = 4$ bases of ResNet-18 from random initialization (different from Sec. 6 that use a pre-trained one that each basis model starts from the same initialization). To evaluate the model’s personalized performance and general quality, we report personalized accuracy and global accuracy defined in Eq. (A); both are averaged over clients.

Method	every iteration	every 5 epochs		
Evaluation	Personalized	Global	Personalized	Global
Test Accuracy	90.2	66.0	69.0	68.8

D More results and discussion

D.1 Additional details and analyses of the bases collapse problem in Sec. 4.3

In Sec. 4.3 and Fig. 2 of the main paper, we presented a PFL experimental result to showcase the bases collapse problem of the baseline training algorithm (cf. Eq. (5) and Eq. (6)). Here, we provide additional details and analyses that we omitted in the main paper due to the page limit.

Brief experimental setup. We use the PACS (Li et al. 2017) dataset, which contains in total 7K training images from 7 classes. We follow the procedure detailed in Sec. 5 to split the training images into $M = 40$ non-IID clients. Each client has images from one of the four domains (Photo, Art, Cartoon, Sketch); the class distribution $\mathcal{P}_m(y)$ of each client m is sampled from a Dirichlet(0.3) distribution to make it skewed and not identical among clients (Hsu, Qi, and Brown 2019). We use $K = 4$ bases and model each by a ResNet-18 (He et al. 2016). We apply the block-wise combinations introduced in Appendix B.2 to increase the representation power of the bases: different blocks are expected to capture different relationships of the image domains and class distributions jointly. Different from the main studies in Sec. 6, to better measure the bases collapse problem, each basis model is randomly initialized rather than starting from the same pre-trained model. We train with the number of rounds equal to 100 epochs overall, using the same training setups described in Appendix B.3.

Evaluation. We consider two cases in which a model could perform poorly in a PFL setting: **1**) it suffers over-fitting, or **2**) it suffers under-fitting; i.e., not well-personalized to each client’s data distribution. We adopt two evaluation metrics to better contextualize the quality of the trained model. First, we follow the PFLBED procedure in Sec. 5 to prepare for each domain a “class-balanced” test set and re-weight it with $\mathcal{P}_m(y)$ to calculate the personalized accuracy for client m . (As a reminder, each client has data from one single domain.) Second, we disregard the re-weighting step but directly evaluate each personalized model using the “class-balanced” test set of its corresponding domain. (That is, we directly calculate the performance on the global test set assigned in step 2 of the PFLBED procedure in Sec. 5 for each client model, without any re-weighting.)

Without loss of generality, let us assume that each test set has the same number of test images N_m , and each test sample is indexed by j . The two metrics mentioned above can be formulated as:

$$\begin{aligned}
 \text{Personalized accuracy:} & \quad \frac{1}{M} \sum_m \frac{\sum_j \mathcal{P}_m(y_j) \mathbf{1}[y_j = h_{\theta_m}(\mathbf{x}_j)]}{\sum_j \mathcal{P}_m(y_j)}, \\
 \text{Global accuracy:} & \quad \frac{1}{M} \sum_m \frac{1}{N_m} \sum_j \mathbf{1}[y_j = h_{\theta_m}(\mathbf{x}_j)]. \tag{A}
 \end{aligned}$$

The personalized accuracy weighs each test sample by $\mathcal{P}_m(y_j)$ to reflect the class distribution of client m ’s training data. This can be considered the standard personalized accuracy in literature. The global accuracy, in contrast, treats each test sample of client m ’s domain equally. To summarize the accuracies of clients, we simply take the average over their accuracy.

Next, we consider the baseline training algorithm in Eq. (5) and Eq. (6) for training our FEDBASIS architecture with different communication frequencies.

Unlimited communication. In terms of the number of local gradient steps per round and the number of total rounds (fixed to 100 epochs of updates), we first consider an *ideal* case: unlimited communication. This allows us to perform global aggregation as soon as we can; i.e., after each mini-batch SGD step. This training procedure very much recovers the conventional centralized training.

Limited communication. In practice, due to communication constraints, it is infeasible to perform global aggregation after each mini-batch SGD step. The standard FL setting is constrained by communication frequency due to the network transmission overload; clients typically can only communicate once after epochs of local SGD steps. We thus study the standard case (McMahan et al. 2017), performing local training for a few (5 here) epochs per round. Tab. A summarizes the results. We have the following observations.

- With unlimited communication (the “every iteration” column), FEDBASIS achieves strong personalized accuracy, much higher than the global accuracy. In other words, under the ideal case, we justify 1) the capacity of our convex combination representation and 2) the capability of the baseline training algorithm for producing personalized models dedicated to each clients’ individual distributions.

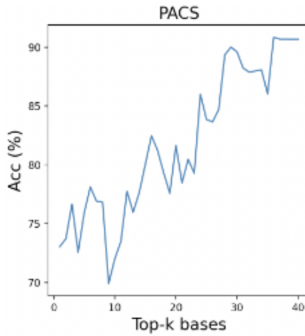


Figure E: Reducing 40 fine-tuned personalized models into top- k bases by PCA.

- With limited communication (the “every 5 epochs” column), FEDBASIS in the more standard FL setting can no longer match the personalized accuracy in the unlimited communication setting.
- To our surprise, under the limited communication scenario, the personalized accuracy is comparable to the global accuracy. Namely, the constructed personalized models do learn good general knowledge (thus not over-fitting) but fail to personalize since they seem almost identical among clients.

These observations motivate our study and analyses in Sec. 4.3. As confirmed in Fig. 2, FEDBASIS by baseline training collapses to non-specialized bases and uniform combinations. In Fig. 2, we found that both the pairwise similarity and the entropy increase along with local training iterations and training rounds. We thus resolve the bases collapse issue by the proposed improved training algorithm in Eq. (8).

D.2 Other baselines: Principal Component Analysis (PCA) and k -means clustering

Our FEDBASIS architecture is to represent personalized models by a set of few basis models. Here, we present another baseline, building upon a reverse way of thinking: *How can we summarize many personalized models into combinations of a few basis models given the federated constraint that no data are available at the server?* A straightforward way to achieve such model compression is to perform Principal Component Analysis (PCA) on the collection of all the personalized models. That is, we can represent each personalized model by the top- k principal components (as $\{\mathbf{v}_1, \dots, \mathbf{v}_k\}$) found by PCA.

We follow the experimental setup in Appendix D.1 to construct 40, non-IID clients. We consider an *ideal* case of personalization in the unlimited communication setting. We first train a global model with mini-batches SGD, and then fine-tune it on each client’s dataset to obtain 40 personalized models $\{\theta_m\}$. Then, we perform PCA on their vectorized parameters.

As shown in Fig. E, we observe that the averaged personalized performance drops drastically as the number of eigenvectors decreases. For instance, using only the top-4 bases leads to slumps in the accuracy of 18.1% for PACS. It demonstrates the challenge of this problem. We hypothesize that the poor performance is likely due to (1) personalized models produced by fine-tuning do not simply lie on a low-dimensional subspace and/or (2) PCA in the model parameters cannot guarantee that the reconstructed models maintain their accuracies. More specifically, PCA aims to minimize the difference between the original models and the reconstructed models in their model parameters, not their accuracies on the personalized test data. As a result, we can observe some fluctuations in accuracy along with the changes in the value k .

Alternately, we investigate using k -means clustering on the personalized models $\{\theta_m\}$ parameters to cluster them into $k = 4$ models and use each client’s assigned centroid as the personalized models. We again see a significant accuracy drop of 21.4% for PACS.

Therefore, we are motivated to solve our proposed objective Eq. (3) that aims to directly learn the bases such that all personalized models can be their linear combinations while minimizing the local empirical risks.

D.3 More results about the robustness of FEDBASIS

In both Tab. 2 in the main paper, we demonstrate the robustness of the FEDBASIS on the choices of stopping epochs when it is fine-tuned for new clients, compared to other baselines. Note that, in the current Tab. 2, for each method and each dataset, we highlight the difference ($|\Delta|$) between stopping the fine-tuning by the last epoch or by the best epoch selected by validation. In Fig. 4, we further compare the best baseline PER-FEDAVG+FT with different learning rates. We observe FEDBASIS is clearly more robust to hyperparameters such as the learning rates and stopping epoch. We focus on the more challenging datasets Office-Home with the small training size setting. In Fig. F, we plotted out the dynamics of the federated training and regularized fine-tuning on new clients, both demonstrating the effectiveness of our FEDBASIS. We attribute it to the clear advantage that FEDBASIS only needs to personalize much fewer parameters when adapting to a new client, thus enjoying the robustness. We further note for PER-FEDAVG+FT, although with proper tuning it can achieve decent performance (still lower than ours), this requires a validation set for each client thus likely not practical in the real world.

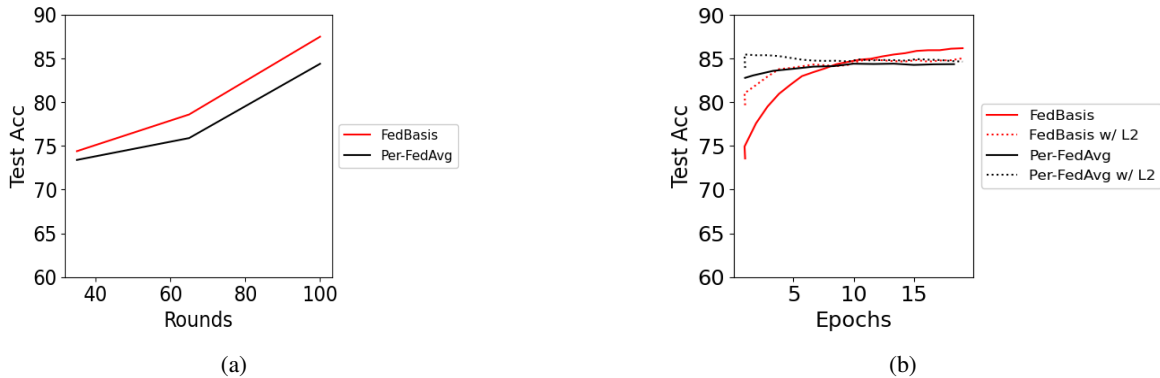


Figure F: (a) Federated training curves of Office-Home (small) dataset (Tab. 2 in the main paper) of PER-FEDAVG+FT and FEDBASIS along the rounds. In each evaluated round (note that FEDBASIS warm-starts from 30 rounds of FEDAVG, as described in Appendix B.2), we run the adaption procedure to evaluate the new clients to report the averaged personalized accuracy as the same as Tab. 2. (b) Fine-tuning curves of Office-Home (small) dataset (Tab. 2 in the main paper) of PER-FEDAVG+FT and FEDBASIS with fine-tuning learning rate = 0.005 with the ℓ -2 regularization in Equation 2 of (Dinh, Tran, and Nguyen 2020) (see Tab. 3).

Table B: More results of PER-FEDAVG+FT with first-order (FO) and Hessian-free (HF) variants in (Fallah, Mokhtari, and Ozdaglar 2020). The results on based on Office-Home (Moderate training size).

Method	Learning rates	Last/Best Acc.				
		0.001	0.005	0.01	0.05	0.1
FEDAVG+FT		78.1/78.1	78.2/78.5	70.5/76.6	65.4/75.6	38.1/73.1
PER-FEDAVG+FT (FO)		86.1/86.1	86.1/86.2	65.3/85.4	60.5/83.4	40.1/82.6
PER-FEDAVG+FT (HF)		85.3/85.3	85.5/85.5	63.4/83.6	43.7/81.6	34.8/80.7
FEDBASIS		87.6/87.6	87.5/87.7	87.6/87.7	87.6/87.6	87.5/87.6

D.4 Extended comparisons and results of Tab. 2

Variants of PER-FEDAVG. In Sec. 6, we focus on the first-order (FO) version of PER-FEDAVG+FT (Fallah, Mokhtari, and Ozdaglar 2020) due to its better accuracy and training efficiency on the datasets in our experiments. In Tab. B, we provide a comparison on PER-FEDAVG+FT with the two variants FO and Hessian-free (HF) introduced in (Fallah, Mokhtari, and Ozdaglar 2020) and we confirmed FO is better in the performance.

Further fine-tuning as personalization components. In Sec. 6, we consider personalization for new clients using the proposed way of each method. Here we provide more complete results (due to the limited space in the main paper) by further considering fine-tuning the classifiers (as linear probe) or the whole model (full fine-tuning, FL in short). As shown in Tab. C, overall FEDBASIS still performs the most competitively in terms of accuracy and robustness. Overall, although linear probes are sometimes more robust than full fine-tuning, full fine-tuning can typically outperform linear probes with proper validation. FEDBASIS somewhat provide a nice balance for such a dilemma since it already learns to personalize by basis composition in the training phase, thanks to the expressive power of non-linear deep neural networks.

Random seeds variances of Tab. 2. We provide the variances of 3 different runs with different random seeds in Tab. D due to the limited space in the main paper.

Effects of numbers of bases K . We study the effects of numbers of bases K . We follow the experiments in Tab. 2 to use the small local size and select the stopping epoch by validations. As shown in Tab. E, a small number of bases is enough to accommodate the personalized variation among the clients, thanks to the effective training in FEDBASIS that enforce the bases to learn to be expressive for combining into different personalized models.

Ablations. We show in Tab. F that our major basis introduced in Appendix B.2 improves the performance, along with other designs we proposed in Sec. 4.3.

Table C: More comprehensive results of Tab. 2 with further personalization. **LP**: further training for a personalized linear classifier. **FT**: further fine-tuning for the whole model. Averaged personalized test accuracy (%) on class non-IID new clients sampled from Dirichlet(0.3). Each method is learned on each client's training data of different sizes for 20 epochs with a learning rate selected from {0.005, 0.01, 0.05}. We report both the **Last** epoch and the **Best** by validation.

Method/Dataset	PACS				Office-Home				GLD23k												
	Training Size		S	M	S	M	S	M	S	M	L										
Epoch	Last	Best	$ \Delta $	Last	Best	$ \Delta $	Last	Best	$ \Delta $	Last	Best	$ \Delta $	Last	Best	$ \Delta $	Last	Best	$ \Delta $			
FEDREP+LP	87.4	87.4	0.0	92.5	92.4	0.1	75.6	75.6	0.0	76.0	76.1	0.1	75.7	77.6	1.9	78.8	78.8	0.0	80.1	80.8	0.7
FEDREP+FT	89.8	89.8	0.0	92.4	92.5	0.1	74.2	76.1	1.9	75.2	76.4	1.2	79.2	79.9	0.7	81.5	82.5	1.0	81.5	83.5	2.0
FEDBN+LP	86.2	88.2	2.0	92.4	92.4	0.0	76.9	77.0	0.1	78.1	78.1	0.0	74.1	74.5	0.4	76.6	76.6	0.0	76.4	76.5	0.1
FEDBN+FT	90.8	92.1	1.3	93.0	93.1	0.1	82.3	82.5	0.2	79.0	79.2	0.2	68.1	70.5	2.4	77.8	81.8	4.0	80.5	83.9	3.4
PFEDHN	85.4	-	-	85.5	-	-	74.1	-	-	74.3	-	-	74.5	-	-	75.6	-	-	77.2	-	-
PFEDHN+LP	90.4	90.4	0.0	90.6	90.6	0.0	75.1	75.1	0.0	77.4	77.4	0.0	77.0	77.6	0.6	78.5	78.5	0.0	79.1	79.5	0.4
PFEDHN+FT	90.5	91.2	0.7	90.4	91.4	1.0	76.2	77.2	1.0	77.1	77.6	0.5	77.6	81.4	3.8	78.6	81.6	3.0	80.2	82.2	2.0
PER-FEDAVG+FT	95.4	95.6	0.2	96.2	96.3	0.1	84.3	84.4	0.1	86.1	86.2	0.1	78.5	85.3	6.8	79.9	85.2	5.3	82.2	86.1	3.9
KNN-PER	71.6	-	-	71.6	-	-	50.4	-	-	54.5	-	-	54.0	-	-	57.4	-	-	69.2	-	-
KNN-PER+FT	72.7	72.7	0.0	79.4	79.7	0.3	51.6	52.4	0.8	54.2	54.4	0.2	54.2	54.5	0.3	57.1	57.8	0.7	69.5	70.2	0.7
FEDAVG	88.1	-	-	88.1	-	-	73.1	-	-	73.1	-	-	45.4	-	-	45.4	-	-	45.4	-	-
FEDAVG+LP	88.2	90.1	1.9	90.5	90.5	0.0	76.6	76.6	0.0	77.0	77.0	0.0	80.8	81.5	0.7	80.9	81.8	0.9	83.3	83.3	0.0
FEDAVG+FT	86.1	91.9	5.8	90.5	90.5	0.0	76.1	77.4	1.3	78.2	78.5	0.3	81.5	84.2	2.7	81.6	84.5	2.9	84.1	86.1	2.0
FEDBASIS	95.2	95.2	0.0	96.2	96.2	0.0	87.4	87.5	0.1	87.5	87.7	0.2	87.4	87.4	0.0	87.6	87.6	0.0	89.0	89.1	0.1

Table D: Variance (σ^2) of personalized test accuracy (%) over 3 different runs for Tab. C.

Method/Dataset	PACS				Office-Home				GLD23k							
	Training Size		S	M	S	M	S	M	S	M	L					
Epoch	Last	Best	Last	Best	Last	Best	Last	Best	Last	Best	Last	Best	Last	Best	Last	Best
FEDREP+LP	0.22	0.16	0.21	0.22	0.31	0.26	0.33	0.25	0.55	0.56	0.47	0.52	0.44	0.29		
FEDREP+FT	0.36	0.29	0.41	0.38	0.66	0.56	0.71	0.39	0.78	0.89	0.88	0.75	0.74	0.71		
FEDBN+LP	0.15	0.16	0.31	0.15	0.12	0.23	0.28	0.19	0.36	0.41	0.29	0.21	0.51	0.39		
FEDBN+FT	0.33	0.45	0.41	0.42	0.67	0.59	0.55	0.62	0.68	0.66	0.56	0.48	0.65	0.62		
PFEDHN	0.78	0.64	0.56	0.57	0.46	0.51	0.48	0.55	0.41	0.28	0.55	0.56	0.39	0.28		
PFEDHN+LP	0.36	0.44	0.29	0.36	0.27	0.31	0.28	0.25	0.87	0.86	0.82	0.75	0.78	0.58		
PFEDHN+FT	0.85	0.97	0.56	0.77	0.77	0.75	0.64	0.70	1.01	1.12	0.89	0.88	0.91	1.15		
PER-FEDAVG+FT	0.51	0.46	0.37	0.41	0.70	0.61	0.63	0.66	0.51	0.25	0.48	0.45	0.34	0.38		
KNN-PER	0.30	0.34	0.19	0.38	0.56	0.58	0.52	0.57	1.14	1.56	1.28	0.85	0.95	0.95		
KNN-PER+FT	1.75	1.41	1.25	1.39	0.57	0.60	0.78	0.69	0.27	0.56	0.48	0.71	0.55	0.61		
FEDAVG	0.23	0.25	0.29	0.24	0.38	0.41	0.50	0.42	0.54	0.39	0.55	0.56	0.54	0.27		
FEDAVG+LP	0.15	0.21	0.20	0.17	0.29	0.22	0.31	0.44	0.63	0.65	0.48	0.59	0.64	0.59		
FEDAVG+FT	0.52	0.39	0.44	0.51	0.57	0.46	0.60	0.58	0.68	0.71	0.59	0.58	0.61	0.48		
FEDBASIS	0.52	0.56	0.45	0.50	0.38	0.39	0.42	0.45	0.52	0.66	0.47	0.68	0.29	0.45		

Table E: Effects of number of bases K in FEDBASIS. We use the small local size and select the stopping epoch by validations, according to Tab. 2.

K	PACS		Office-Home		
	1	2	4	6	8
1	91.9	77.4			
2	93.4	84.5			
4	95.2	87.5			
6	94.7	87.6			
8	95.0	87.4			

Table F: Ablation studies of FEDBASIS designs in Sec. 4.

Coordinate	Descent	Major	Basis	τ	Office-Home	GLD
✗	✓	✓	✓	0.1	83.5	85.8
✓	✗	✓	✓	0.1	87.2	83.3
✓	✓	✗	✓	1.0	87.1	85.5
✓	✓	✓	✗	0.1	87.5	87.6